Object Description and Decomposition by Symmetry Hierarchies

Kai Huebner
Safe and Secure Cognitive Systems
German Research Center for Artificial Intelligence
D – 28359 Bremen, Germany
kai.huebner@dfki.de

ABSTRACT

Symmetry is an important feature of visual scene exploration and interpretation. Similarly, hierarchical structures figure an important aspect of symmetry. Visual symmetries describe image regions that might naturally overlap or enclose smaller symmetries. For this reason, objects and scenes can be described in their overall shape as also in their decomposition into more detailed subordinate structures by symmetry hierarchies. Most hierarchical approaches in this area are based on structural, multi-scalar or multi-resolution hierarchies. In this paper, we propose a symmetry-oriented hierarchy with a related, but more cognitive meaning by describing a hierarchy of symmetry itself based on a range-based symmetry detector. We motivate and present an approach for symmetry hierarchy representation and show experiments towards object description and decomposition by symmetry hierarchies.

Keywords

Bilateral Symmetry Detection, Symmetry Hierarchies, Object and Scene Description.

1. INTRODUCTION

Symmetry has been investigated in several domains like biology, psychology and computer vision. In nature and human perception, symmetry is a widespread feature. Most artifacts are built in a symmetric manner and both animals and humans use symmetry as a significant landmark. Besides this property, psychophysical work [PH78, LN89] shows that especially vertical symmetry (i.e. reflective symmetry with respect to a vertical axis) is the fastest and most accurate detectable for the human eye. Assuming the presence of bilateral symmetry in a scene, humans are able to immediately detect symmetry axes for further visual exploration of the scene or for interaction with the real world. Accordingly, symmetry is also applied as a valuable attentional feature for the extraction of regions of interest or for object description by symmetric properties in the area of computer vision [RWY95, DV95, ZPA95]. Though mainly reflective symmetries are used, approaches to rotational symmetries can also be found in the literature [LZ03].

Hierarchical structures figure an important aspect of symmetry. Symmetries normally describe feature regions that cover larger image parts than local features such as edges or corners. Therefore, one symmetry region might naturally overlap or enclose further, but smaller symmetry regions. For this reason, objects and scenes can be described in their overall shape as also in their decomposition into more detailed subordinate structures by symmetry hierarchies. This idea is illustrated for the building scene in Figure 1. The building is highly bilateral symmetric as a whole, but moreover, it encloses several symmetrical substructures like those depicted in the illustration.

On the other hand, symmetry hierarchies allow to analyze symmetries in different levels of granularity. This is an important issue, as many objects such as faces or trees appear symmetrical when visualized with low res-

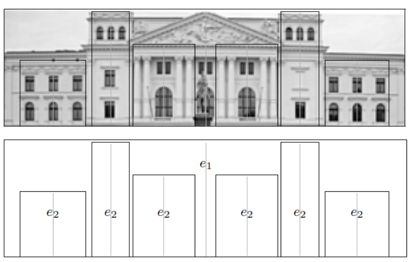

Figure 1: A building and some of its intuitive symmetrical substructures.

ISBN 978-80-86943-02-2

olution. However, these objects are not that symmetric in high resolution, e.g. when we focus on object details like crinkles or branches. Zabrodsky *et al*. motivated this idea of hierarchically ordered symmetry detectors in [Zab90] and [ZPA92].

In this paper, we present a novel symmetry hierarchy algorithm based on our previous work on a quantitative (i.e. range-based) symmetry detector. Approaches from the literature focus on the structure of the hierarchy with regard to operator size or image size. Related work and the classification of hierarchies are discussed in sections 2 and 3. In contrast to these methods, our quantitative detector provides a novel kind of symmetry-oriented hierarchy. Section 4 includes the hierarchy algorithm, section 5 shows an experimental application. We conclude our work in section 6.

2. RELATED WORK

Hierarchical Symmetry

The most intuitive way to realize the idea of symmetry hierarchies is to hierarchically structure the symmetry detectors themselves. Di Gesù and Valenti formulate the Pyramid Discrete Symmetry Transform in [DV97]. The resulting hierarchy is pyramidal, as a quadtree is used to represent the different levels of symmetry granularity. Kelly and Levine apply annular operators of variable size to detect and group symmetries belonging to their size in [KL95]. The different layers of the vector field representation by Cross and Hancock [CH99] also allow the detection of variably scaled symmetry axes.

In earlier work [ZH02], we combined a set of compact symmetry operators on panoramic images. This was motivated by the observation that the mask-based detector shows different pros and cons depending on the size of the operator. Though the extraction of symmetry axes is more robust with the use of multiple operators, it is comparatively slow and inefficient. Within all of the referred approaches, a variable parameter of detector scale is included. A symmetry hierarchy of an object can therefore not be established until a multi-scale computation of the detector has been performed. It is obvious, that this processing of several scales strongly increases the efforts in computation time.

Quantitative Symmetry

A novel method to generate robust range-based symmetry values was proposed in [HWZ05]. The approach is based on an algorithm computing bilateral quantitative symmetry information using an adopted Dynamic Programming technique referred to as Dynamic Programming Symmetry (DPS) algorithm. For each image point, the pair of opposing image regions spans a single local search space. Each search space is computed to find an optimal mapping of the regions' elements. Symmetry information is finally extracted regarding the error of this mapping.

The optimal mapping and the overall error are computed in an iteratively growing subsquare of the search space. The optimized procedure and the successive iteration steps including the determination of the symmetry values $sigma_L$ and $sigma_R$ are presented in Fig. 2.

If the minimum error exceeds a given threshold in an iteration step, the calculation is aborted. The mapping end is returned by its search space indices $\sigma_L(p_i)$ and $\sigma_R(p_i)$ that now serve as a measure of symmetry. The environment given by $S = \sigma_L(p_i) + \sigma_R(p_i)$ can be treated intuitively as the symmetric region around p_i. Thereby, the operator offers comparable symmetric range information, referred to as *quantitative* symmetry, for each image point.

The disadvantage of this approach is the high effort in computing time, as a whole search space has to be treated for each pixel. An illustration taken from that work is Fig. 3. The re-use of particular cells is pointed out by their shading. As can be seen, both path structures and the overall error are not transferable because of the networked minimization strategy that is used in the different local search spaces. A detailed description and optimization of the Dynamic Programming Symmetry algorithm and its usability based on quantitative symmetry signatures for motion tracking can be found in [HWZ05].

Hierarchical Structures

Inside the approaches to hierarchical symmetry that were mentioned above, the term of a "hierarchy" describes ordered structures related to the technical processing of symmetries. Each of these resembles a structural hierarchy of the applied detectors. However, this is only one of several types of "hierarchies" which we distinguish and describe in the following.

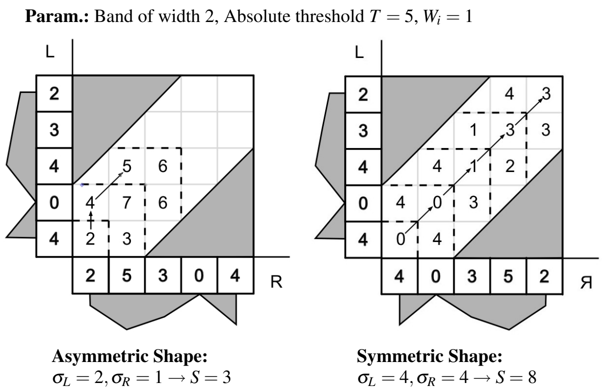

Figure 2: DPS-Algorithm: The difference between asymmetric and symmetric local search spaces is visible. Costs and mapping path differ clearly.

 ISBN 978-80-86943-02-2

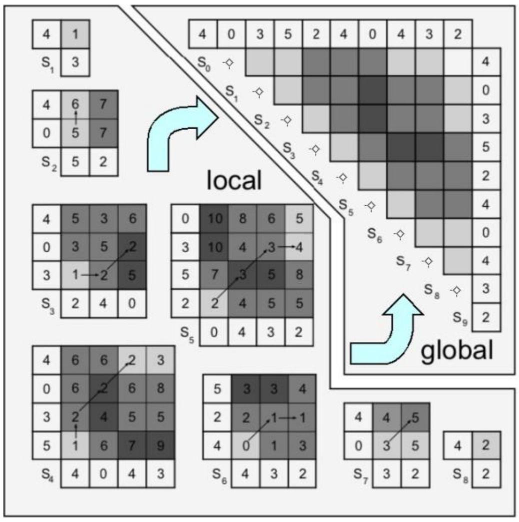

Figure 3: Local square search spaces and combination of the local search spaces into a triangular global search space [HWZ05]. Note that paths and values differ in overlapping local search spaces.

2.3.1 Multi-Scalar Hierarchies

Multi-scalar hierarchies are characterized by the utilization of several differently scaled detectors. Hence, the term of "hierarchy" primarily describes the hierarchy of detectors, but not the hierarchy of symmetries. On the one hand, a small set of larger detectors maybe applied first to subsequently focus more detailed regions with smaller detectors (top-down principle). On the other hand, small detectors maybe applied first before subsequently analyzing symmetric regions with enlarged detectors (bottom-up principle). The detectors from [KL95], [CH99] and [ZH02] are examples for this type of hierarchies that build up a hierarchy $H(I)$ of an image I by applying a symmetry detector Θ with manifold operator sizes $m_{1...n}$:

$$\{\Theta(I, m_n)\} \Rightarrow H_{ms}(I),\ n \in \mathbb{N}^+. \quad (1)$$

2.3.2 Multi-Resolution

The approach of multi-resolution follows a different motivation. Many objects may appear symmetric as a whole, but show inaccuracies when analyzed in detail. Therefore, multi-resolution considers the image in different levels of resolution. Thus, the parameter in this case is the resolution of the image and not the size of the operator, as it is in multi-scale approaches. By the order of different resolutions, the term of "hierarchy" also describes a structural hierarchy of resolutions instead of a hierarchy of symmetries:

$$\{\Theta(I_n, m)\} \Rightarrow H_{mr}(I),\ n \in \mathbb{N}^+. \quad (2)$$

Examples for symmetry multi-resolution are described by Zabrodsky *et al*. [Zab90, ZPA92] and Di Gesù and Valenti [DV97].

2.3.3 Symmetry-Oriented Hierarchies

Within the context of the method to detect quantitative symmetry, the term of a hierarchy finds a related, but more cognitive meaning. The symmetry-oriented hierarchy does not focus on the structure of the hierarchy in reference to operator size (multi-scalar) or image size (multi-resolution). Instead, it describes a hierarchy of symmetries itself, like the one illustrated in Figure 1. This type of hierarchy is only feasible with quantitative symmetry information like provided by the DPS (Dynamic Programming Symmetry) algorithm, but it allows symmetry hierarchies without consideration of a structure of operators:

$$\Theta(I) \Rightarrow H_{so}(I). \quad (3)$$

3. SYMMETRY HIERARCHIES

Quantitative Hierarchy Algorithm

The opportunity to establish hierarchies of symmetries is a fundamental advantage of quantitative symmetry detection. The DPS algorithm assigns a symmetric range to each image point. Thereby, the recognition of hierarchically ordered symmetry structures is strongly supported. The effort for complex analysis and combinations of mutliple-scale operators known from qualitative approaches is not necessary here. One-dimensional symmetric range information allows the construction of symmetry hierarchies by simple interval calculation.

Symmetry axes are detectable at maxima values in quantitative symmetry images. From these points, symmetry values decrease constantly. Thus, higher-level symmetries are depicted as global maxima values in intervals. Lower-Level symmetries can be found at local maxima inside these intervals. The following recursive algorithm to reveal the hierarchical symmetry structure is therefore both intuitive and effective. Calculations are based on one-dimensional intervals T:

1. Find in $T = [l, r]$ the global, margin-independent maximum σ^s (with index s and symmetry range values $\sigma_L(s)$, $\sigma_R(s)$).

2. Mark s as a symmetry of hierarchical order e.

3. Set four partial intervals as follows:
- **3.1** $T^{ol} = [l,\ \max(l,\ s - \sigma_L(s))[$ (outer-left interval)
- **3.2** $T^{il} = [\max(l,\ s - \sigma_L(s)),\ s[$ (inner-left interval)
- **3.3** $T^{ir} =]s,\ \min(s + \sigma_R(s),\ r)]$ (inner-right interval)
- **3.4** $T^{or} =]\min(s + \sigma_R(s),\ r),\ r]$ (outer-right interval)

4.1 For T^{ol} and T^{or} repeat the algorithm ($\rightarrow$ **1.**) with hierarchical order e (equivalent level of hierarchy).

4.2 If $e < e^{max}$, i.e. the maximum hierarchy level is not reached, repeat the algorithm ($\rightarrow$ **1.**) for T^{il} and T^{ir} with hierarchical order $e + 1$ (subordinate level of hierarchy).

 ISBN 978-80-86943-02-2

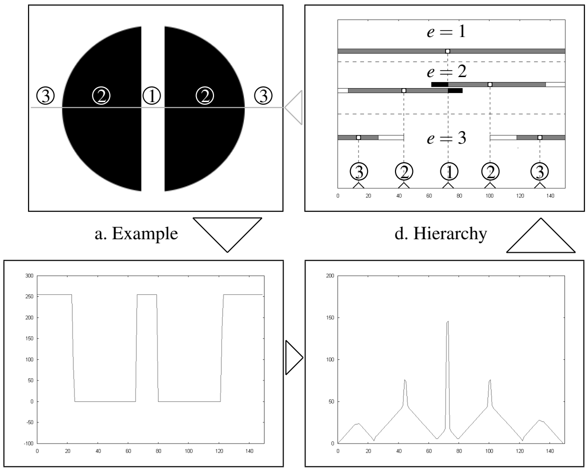

a. Example d. Hierarchy

b. Grayscale Pattern (center row) c. Overall symmetry $\sigma = \sigma_L + \sigma_R$

Figure 4: Steps of symmetry hierarchy algorithm.

We set T as the whole image row in the first recursion step. Additionally, a maximal recursion depth and hierarchy sub-level, respectively, is given by e^{max}. Hereby, a hierarchy structure of an image row can be established like the one presented in Figure 4.

Regarding the concluding "hierarchy" in Figure 4d, the bars correspond to the symmetric intervals of the symmetry maxima depicted by points. The inner intervals T^{il} and T^{ir} are illustrated by gray bars, the outer intervals T^{ol} and T^{or} by white bars. Black bars correspond to interval overlaps caused by the symmetry ranges σ_L and σ_R, respectively. Following the interval definition, these overlaps are not further processed. Finally, the interval gaps that are depicted in level $e = 3$ do not include margin-independent maxima.

The proposed algorithm allows detection of symmetry axis points and their interval-based classification into a symmetry hierarchy. Symmetry information of an image can thereby be reduced to symmetry axes which still represent meaningful information. In addition to the assignment of a range-based symmetry value, each image point can be classified as a symmetry axis point, including its rank in a symmetry hierarchy.

Row-Oriented Hierarchies

For vertical symmetries, both the DPS algorithm and the hierarchy algorithm work on local, single image rows. A row-spanning combination of the local hierarchy points into symmetry segments allows higher-level description of an image's symmetry structure. In the following, we show a column-based combination to show up the usefulness of more global symmetry hierarchy descriptions. The processing steps are: symmetry detection (DPS algorithm), row-based detection of symmetry axes including their hierarchy levels (hierarchy algorithm), histogram of the hierarchy levels.

The examples of Figure 5 show different vertical symmetry structures produced by the row-based algorithm. Both hierarchies of the first level (c,d) build a nearly centered vertical main-axis, as both images are strongly vertical symmetric. Accordingly, the symmetry values are high in this first hierarchy level. However, the symmetry maxima of the second level (e,f) show differences. The circle (a) shows two arcs for the symmetry structure of the black semi-circles for $e = 2$ (e) that are both subordinate to the center symmetry of $e = 1$ (c). However, the curvature of the arcs shows just a small effect on the column-histogram presented at the bottom. The building (b) allows further interesting observations. The main symmetry on top level $e = 1$ (d) is significant, but does not span the whole image because of image noise. Thus, the algorithm produces further first-level symmetry axes. Below the first level, the branching of symmetry axis are clearly visible up to the third level ($e = 3$) of the histogram (h). We can detect symmetries of first level for the building's center part, the two towers and the two window fronts, symmetries of second level for the building columns and window pairs and symmetries of third level for subordinate window parts. This symmetry hierarchy and its parts are illustrated in Figure 6.

Histogram-Oriented Hierarchies

In Figure 6, the selection of maxima was made manually for the row-oriented hierarchy. The image parts were then extracted using these maxima and the corresponding symmetry ranges. An automatic detection of the depicted histogram structure may surely be realized. However, this would include a maxima detection about each local image row and further parametrization and tuning of the algorithm.

Instead of following the row-based approach, we concentrate on a histogram-oriented one. We therefore change the order of the last two processing steps, so that these are now: symmetry detection (DPS algorithm), histogram of the symmetry values, row-based detection of symmetry axes including their hierarchy levels (hierarchy algorithm). The disadvantage of this method is that the exact symmetry ranges σ_L and σ_R are lost by calculating each column's mean symmetry value. The mean ranges

$$\hat{\sigma}_L(x) = \frac{1}{h}\sum_{y=0}^{h-1}\sigma_L(x,y) \quad \text{and} \quad \hat{\sigma}_R(x) = \frac{1}{h}\sum_{y=0}^{h-1}\sigma_R(x,y) \tag{4}$$

are therefore sensitive to changes. The mean symmetry value is only equal to the exact symmetry range if symmetry is equal throughout the whole column.

The mean histogram that is extracted by this step is now processed by the recursive algorithm to build the histogram-based symmetry hierarchy of the image.

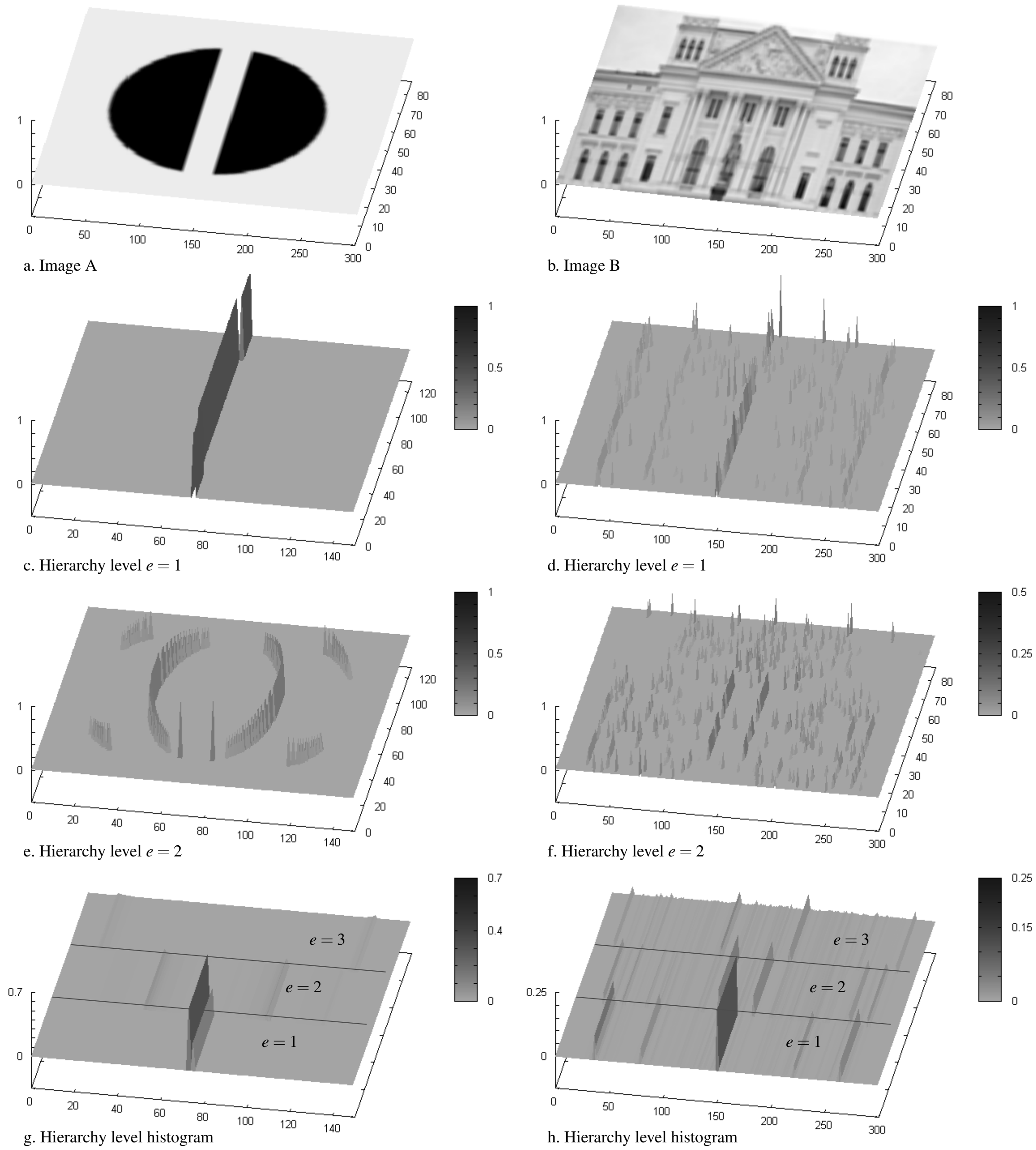

a. Image A
b. Image B
c. Hierarchy level $e = 1$
d. Hierarchy level $e = 1$
e. Hierarchy level $e = 2$
f. Hierarchy level $e = 2$
g. Hierarchy level histogram
h. Hierarchy level histogram

Figure 5: Two examples for the symmetry-based hierarchy description. Top to bottom: source images (a,b); row-based vertical hierarchies of levels $e = 1$ (c,d) and $e = 2$ (e,f); corresponding symmetry level histograms (g,h). The z-values depict which portion of the image is covered by the symmetry, i.e. it is $z = 1$ if the whole image is covered by that symmetry.

While the hierarchy algorithm has to be applied for each row in the row-based approach, it has to be used only once here. Regarding the example, this automatic algorithm yields a good result especially in the first hierarchy level $e = 1$ (see Figure 7). Note that this result is very similar to the intuitive decomposition of a hierarchy structure that was discussed in Figure 1 in the introduction.

4. EXPERIMENT

In our experiment, we exploit the proposed symmetry hierarchy algorithm for panoramic image decomposition. Therefore, we use our mobile robot platform, the Bremen autonomous wheelchair "Rolland III" (see Figure 8) in a common office environment. Image sequences of dynamic environments are quite sensitive to

 ISBN 978-80-86943-02-2

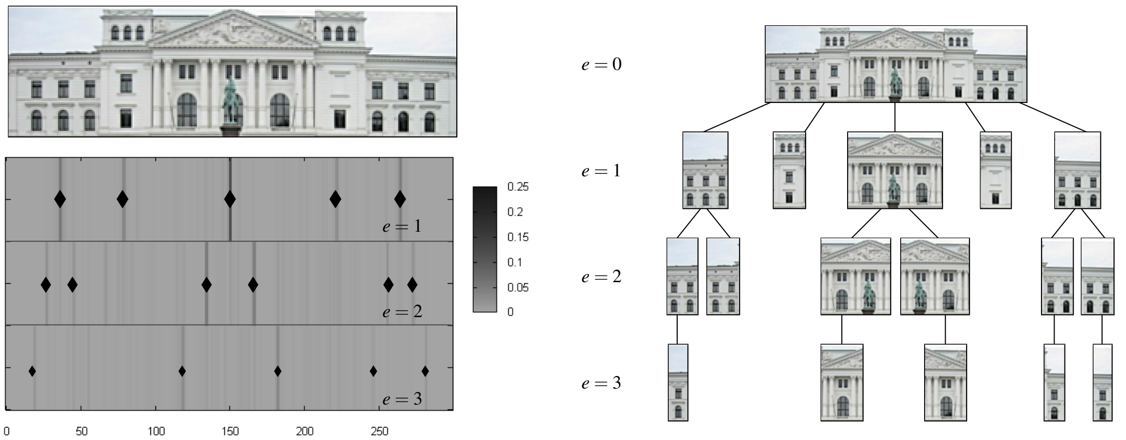

Figure 6: Left: Hierarchy level histogram (same as Figure 5h) with *manually* marked symmetry axes (diamonds). Right: Illustration of the corresponding symmetry-oriented hierarchy, *manually* extracted.

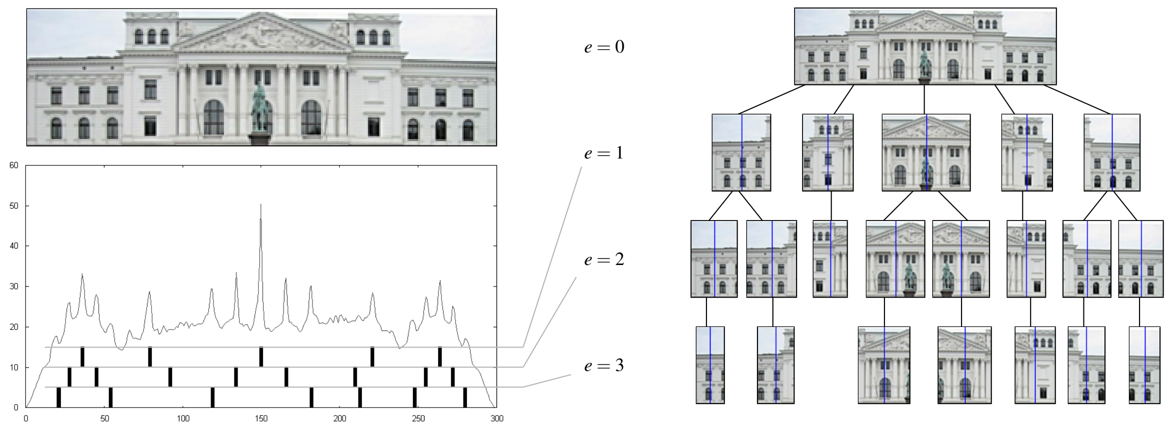

Figure 7: Left: Mean column histogram of all symmetries $\hat{s} = \hat{\sigma}_L + \hat{\sigma}_R$ with *automatically* marked symmety axes (bars). Right: Illustration of the corresponding symmetry-oriented hierarchy, *automatically* extracted.

a multitude of image transformations like scale change, illumination, occlusion and many more. In earlier work [ZHK01], we proposed a sectoring of panoramic images in order to be more robust to those influences. If one of the sectors can not be recognized by the robot because of unexpected occlusion (maybe by a person around), the correct assignment can also be made by the other sectors. In that work, we used a constant sectoring of the panoramic image into three sectors of 90 degree each. In the following experiments, the proposed symmetry hierarchy algorithm will produce arbitrarily-sized sectors. Panoramic images are normalized in orientation, so the only symmetry that is used for hierarchical image decomposition is vertical symmetry (i.e. symmetry about a vertical axis).

Experimental Setup

“Rolland III” is equipped with two Siemens LS4 laser scanners mounted at ground level, which allow for scanning two fields of 190 degrees in front of and backwards of the wheelchair. Two Lenord+Bauer GEL248 incremental encoders measure the rotational velocity of the two independently actuated wheels. Here, we concentrate on the SeiwaPro Panorama Eye® omnidirectional vision system that is mounted at the top of the wheelchair’s backrest. Like most catadioptric systems, the one applied here comprises a firewire color camera facing upwards to a hyperboloidal mirror surface. Omnidirectional images are restricted in image resolution, but offer the main advantage of providing a complete 360-degrees visual perception of the surroundings in each time step. Thus, they are widely applied and researched in robot vision tasks. Methods for unwarping distorted omnidirectional views into both panoramic and perspective views are well elaborated to offer user-friendly visual feedback (see Figure 8).

Experimental Results

The following experiment concentrates on the decomposition and hierarchization of panoramic images only. Some panoramic images are presented in Figure 9.

Both images are made at the same position, but with different orientation. Additionally, the wheelchair

 ISBN 978-80-86943-02-2

Figure 8: The autonomous wheelchair. The camera image (top-right) showing the omnidirectional view can be unwarped into both perspective views (center-right) and into the panoramic view (bottom).

driver and another person occlude arbitrary image parts. Thus, it is obvious that a fixed sectoring of the images would not be useful at all to find correspondences between the image parts.

We now apply the histogram-oriented hierarchy algorithm on both images. For each image, a hierarchical structure of six sectors is automatically produced and shown in Figure 10. Decomposition is only done up to first level of hierarchy, sub-ordinate levels are not used. As can be seen, the panoramic images are divided into sectors that are symmetrically significant. We also find that they show object-bound parts like doors and walls.

To show up that correspondences between these image sectors can now be analyzed, we describe each of the image sectors A_i, B_j by a weighted color histogram. For each sector, color information is weighted according to a normal distribution $\hat{p}$ placed abroad the sector. Thereby, a normalized discrete color histogram describes each sector's content. Two histograms can easily be compared using the Bhattacharyya coefficient

$$\rho\left(A_i, B_j\right) = \sum_{u=1}^{m} \sqrt{\hat{p}_u(A_i)\hat{p}_u(B_j)}, \qquad (5)$$

where u is the bin index of the m-sized color histogram. Table 1 shows all the correspondence values between $A_{1\ldots6}$ and $B_{1\ldots6}$. We find that two correspondences can be robustly made: $A_1 \leftrightarrow B_1$ and $A_6 \leftrightarrow B_3$. In these cases, values are high and differing from the others in the table line and row, respectively. While we know that the wheelchair driver is a constant occlusion in driving direction ($A_1 \leftrightarrow B_1$), the assignment $A_6 \leftrightarrow B_3$ is a correct match of the same door in both images.

	B_1	B_2	B_3	B_4	B_5	B_6
A_1	**.87**	.41	.36	.32	.31	.38
A_2	.38	.42	.37	.35	.42	.88
A_3	.28	.83	.62	.80	.79	.51
A_4	.32	.62	.50	.48	.52	.49
A_5	.63	.54	.42	.37	.42	.81
A_6	.26	.52	**.86**	.69	.66	.35

Table 1: Correspondence values between the sectors $A_{1\ldots6}$ and $B_{1\ldots6}$ presented in Figure 10. The two most robust matches $A_1 \leftrightarrow B_1$, $A_6 \leftrightarrow B_3$ are marked bold. Other values are either too small or too similar for a good match (e.g. $B_6 \leftrightarrow A_2$ is high, but $B_6 \leftrightarrow A_5$ is also, thus B_6 can not be assigned robustly).

5. CONCLUSIONS

We have shown that the DPS algorithm for quantitative symmetry detection offers an adequate fundament for hierarchical structuring of symmetric image information. The global search space representation allows a multi-resolution representation. However, the main impact of this work is found in the purely symmetry-oriented hierarchies. As presented, a simple interval calculation on the quantitative symmetry information yields this type of hierarchy. A row-based and a histogram-based application of this idea have been proposed on vertical symmetry data. Experiments show that an object with normalized orientation can be decomposed into several parts belonging to its symmetrical structure.

For applying this concept to object decomposition, pre-processing steps like segmentation and orientation normalization (e.g. Principal Component Analysis) have to be used. In natural scenes, objects are commonly not normalized in rotation, but randomly positioned and oriented. When a main orientation is given, we can apply the proposed operator to detect symmetry hierarchy structure along or perpendicular to this direction. This result can be used to describe objects and scenes with regard to their symmetric structure.

Finally, we showed the application in a real panoramic image scenario, where the scene orientation is naturally fixed. Using the proposed hierarchy algorithm, we have dynamically split each image into symmetry-based sectors. These can be described and matched to find correspondences of sectors. Occluded or unknown sectors can be found and neglected. In contrast, sectors that are detected and matched robustly in both images can be used for re-orientation.

Future work may concentrate on the combination of the basic concept with symmetry segments or regional features, like those proposed in earlier work [HWZ06, HZ06]. On the one hand, symmetry hierarchies maybe detected inside these oriented, regional and object-bound features, thus pre-processing would be made by the regional feature detection. On the

Figure 9: Top: First image A with occlusion by the wheelchair driver and another person. Bottom: Second image B at same position, but with different orientation and without person.

Figure 10: First level symmetry hierarchy of the panoramic images presented above. Top: sectors $A_1 - A_6$. Bottom: sectors $B_1 - B_6$. The proposed algorithm divides the images into highly symmetric segments.

other hand, regional features maybe parts of hierarchies themselves. By these approaches, the quantitative symmetry algorithm will become more general and applicable towards symmetric description and decomposition by symmetry hierarchies.

REFERENCES

[CH99] A. D. J. Cross and E. R. Hancock. Scale space vector fields for symmetry detection. *Image Vision Computing*, 17(5-6):337–345, 1999.

[DV95] V. Di Gesù and C. Valenti. The Discrete Symmetry Transform in Computer Vision. Technical report, DMA Università di Palermo, 1995.

[DV97] V. Di Gesù and C. Valenti. Detection of regions of interest via the Pyramid Discrete Symmetry Transform. In Solina, Kropatsch, Klette, and Bajcsy, editors, *Advances in Computer Vision*, pages 129–136. Springer, 1997.

[HWZ05] K. Huebner, D. Westhoff, and J. Zhang. Optimized Quantitative Bilateral Symmetry Detection. *Int. Journal of Information Acquisition*, 2(3):241–249, September 2005.

[HWZ06] K. Huebner, D. Westhoff, and J. Zhang. A Comparison of Regional Feature Detectors in Panoramic Images. In *IEEE International Conference on Information Acquisition*, 2006.

[HZ06] K. Huebner and J. Zhang. Stable Symmetry Feature Detection and Classification in Panoramic Robot Vision Systems. In *IEEE/RSJ International Conference on Intelligent Robots and Systems*, pages 3429–3434, October 2006.

[KL95] M. F. Kelly and M. D. Levine. Annular Symmetry Operators: A Method for Locating and Describing Objects. In *Fifth International Conference on Computer Vision*, pages 1016–1021, 1995.

[LN89] P. J. Locher and C. F. Nodine. The Perceptual Value of Symmetry. *Computers and Mathematics with Applications*, 17:475–484, 1989.

[LZ03] G. Loy and A. Zelinsky. Fast Radial Symmetry for Detecting Points of Interest. *IEEE Transactions on Pattern Analysis and Machine Intelligence*, 25(8):959–973, August 2003.

[PH78] S. E. Palmer and K. Hemenway. Orientation and Symmetry: Effects of Multiple, Rotational, and Near Symmetries. *Journal of Experimental Psychology: Human Perception and Performance*, 4(4):691–702, 1978.

[RWY95] D. Reisfeld, H. Wolfson, and Y. Yeshurun. Context Free Attentional Operators: the Generalized Symmetry Transform. *Int. Journal of Computer Vision*, 14:119–130, 1995.

[Zab90] H. Zabrodsky. Symmetry - A Review. Technical report, Department of Computer Science, The Hebrew University of Jerusalem, May 1990.

[ZH02] J. Zhang and K. Huebner. Using Symmetry as a Feature in Panoramic Images for Mobile Robot Applications. In *Robotik 2002*, volume 1679 of *VDI-Berichte*, pages 263–268, Ludwigsburg, 2002.

[ZHK01] J. Zhang, K. Huebner, and A. Knoll. Learning based Situation Recognition by Sectoring Omnidirectional Images for Robot Localisation. In *IEEE Workshop on Omnidirectional Vision*, Budapest, 2001.

[ZPA92] H. Zabrodsky, S. Peleg, and D. Avnir. Hierarchical Symmetry. *International Conference on Pattern Recognition*, C:9–12, 1992.

[ZPA95] H. Zabrodsky, S. Peleg, and D. Avnir. Symmetry as a Continuous Feature. *IEEE Transactions on Pattern Analysis and Machine Intelligence*, 17(12):1154–1166, 1995.